phys. stat. sol. (b) **244**, No. 5, 1478–1482 (2007) / **DOI** 10.1002/pssb.200675145

The phonon dispersion of wurtzite-ZnO revisited

J. Serrano[*, 1], **F. J. Manjón**[2], **A. H. Romero**[3], **A. Ivanov**[4], **R. Lauck**[5], **M. Cardona**[5], and **M. Krisch**[1]

[1] European Synchrotron Radiation Facility, BP 220, 38043 Grenoble cedex 9, France
[2] Dpto. de Física Aplicada, Univ. Politècnica de València, Cno. de Vera s/n, 46022 València, Spain
[3] CINVESTAV, Departamento de Materiales, Unidad Querétaro, Querétaro 76230, Mexico
[4] Institut Laue Langevin, 156X, 38042 Grenoble cedex 9, France
[5] Max-Planck-Institut für Festkörperforschung, 70569 Stuttgart, Germany

Received 4 September 2006, revised 29 January 2007, accepted 1 February 2007
Published online 11 April 2007

PACS 61.12.Ex, 63.20.Dj

Inelastic neutron scattering measurements are reported for the optical phonon branches of wurtzite ZnO. The experimental data are in excellent agreement with the *ab-initio* calculations for the phonon dispersion relations based on linear response theory. Discrepancies between theory and present data observed for the longitudinal optic branches along the [100] and [001] directions are attributed to an inaccurate description of the dielectric constant of ZnO and, consequently, the crystal- and electric-field splitting.

1 Introduction

Wurtzite crystals have become a focus of attention in the last years due to the applications of group-III nitrides for blue lasers [1] and the capabilities to cover the whole visible spectral range by using alloys of GaN, AlN, and InN. ZnO is considered as another potential material for such applications, since it exhibits similar structure and electronic band gap as GaN. The relevance of wurtzite ZnO as a semiconductor suitable for applications in the optoelectronic industry has generated considerable effort towards the growth, characterization, and doping of this material, whose impact can be easily appreciated in a number of dedicated workshops and conference sessions.

Most of the works are focused on the electronic and optical properties of ZnO, the emphasis being placed on the possibility of controlled p- and n-type doping for the production of new optical devices such as light emitting diodes or lasers in the ultraviolet range [2]. However, the thermodynamical properties, among them the specific heat and the heat transport, also play an important role in the understanding of the advantages and limitations of ZnO for such applications. These properties are intimately related to the vibrations of the atomic lattice in the crystal and can be derived semiempirically from the phonon dispersion relations. The knowledge of the phonon dispersion relations of ZnO facilitates the validation of theoretical models for phonon calculations applied to the wurtzite structure, allows the understanding of lattice dynamics in anisotropic crystals, and yields an empirical approximation to the phonon density of states (DOS), which is the master pillar for most thermodynamical properties of semiconductors. The experimental data available on the phonon dispersion relations of ZnO are, however, rather limited. Only the acoustic branches along high-symmetry directions were reported in the sixties by inelastic neutron

* Corresponding author: e-mail: jserrano@esrf.fr

scattering (INS) measurements [3–5]. Moreover, several investigations have been performed for $q = 0$ using Raman scattering [6–9].

We report here INS measurements of acoustic and optic phonon branches in wurtzite ZnO. The experimental data are compared with first principles calculations of the lattice dynamics, which have been reported elsewhere [10].

2 Experimental details

We have conducted INS experiments on a single crystal of ZnO of 30 mm height and 15 mm diameter, oriented along the *c*-axis. Measurements of acoustic and optic branches of the phonon dispersion relations were performed along the main high symmetry directions at the hot source IN1 triple axes spectrometer at the Institute Laue Langevin in Grenoble, France. A He closed-cycle refrigerator was employed to cool the sample down to 10 K in order to reduce anharmonic effects and multiple phonon scattering. Using Soller-slit collimators in the incident and scattered beams, we obtained spectra with an experimental resolution of 4 meV. Typical accumulation times were 20 to 40 minutes for each spectrum. They were obtained using a final momentum $k_f = 65$ nm^{-1}.

3 Calculation details

Theoretical calculations were performed in the framework of the local-density approximation (LDA) of the density functional theory (DFT) as implemented in the ABINIT package [11]. The Kohn–Sham orbitals were expanded in plane waves up to a cutoff of 80 Hartrees for wz-ZnO after explicitly checking total energy convergence up to 0.1 meV/atom. Pseudopotentials were generated using the Troullier–Martins scheme [12]. Integrals over the Brillouin zone were replaced by a sum on meshes of $8 \times 8 \times 4$ points in the irreducible Brillouin zone, following a Monkhorst–Pack scheme. The lattice dynamics were calculated after relaxation of the lattice parameters to the minimal energy structure within the linear response formalism of density functional perturbation theory [13]. The dynamical matrices were calculated for a mesh of *q*-points ($6 \times 6 \times 3$) in the irreducible Brillouin zone and then interpolated to obtain the phonon dispersion relations [14]. More details of the calculations can be found in Ref. [10].

4 Results and discussion

As for any other wurtzite material, the phonon dispersion of ZnO exhibits 12 phonon branches grouped into the $2E_2 + 2E_1 + 2A_1 + 2B_1$ irreducible representations at the Γ-point. The E_1, E_2, and A_1 modes are Raman active, the E_1 and A_1 modes are infrared active, and the B_1 modes are silent, i.e. they cannot be observed with Raman and infrared spectroscopy in perfect single crystals. The E_1 and E_2 modes are doubly degenerated each. One doubly degenerated E_1 mode and one A_1 mode are the acoustic modes whereas the rest are optic modes. The optic E_1 mode splits at Γ into transverse and longitudinal optic (TO and LO) branches due to the macroscopic electric field, and the optic A_1 branch also shows different frequencies when approaching the Γ-point depending on the symmetry direction, thus splitting also onto TO and LO modes. The splitting between E_1 and A_1 modes appears in anisotropic crystals due to the crystal field and has been extensively reported in [15, 16].

Beside the Raman modes, the two-phonon DOS has been partially obtained as well via Raman measurements of the linewidth of the highest E_2 mode under pressure and changing the isotopic composition [17], in excellent agreement with *ab-initio* calculations [10]. The B_1 modes have been observed by Raman spectroscopy in heavily doped ZnO single crystals [18], also in good agreement with the *ab-initio* calculations. Beside these calculations, to our knowledge, there has been just a semiempirical model for the lattice dynamics [5]. The *ab-initio* calculations though fail to describe correctly the phonon frequencies corresponding to the longitudinal optic modes at Γ: the calculated splitting between the E_1^{LO} and the A_1^{LO} is not only smaller than the experimental one, but it has also opposite sign and the splitting between

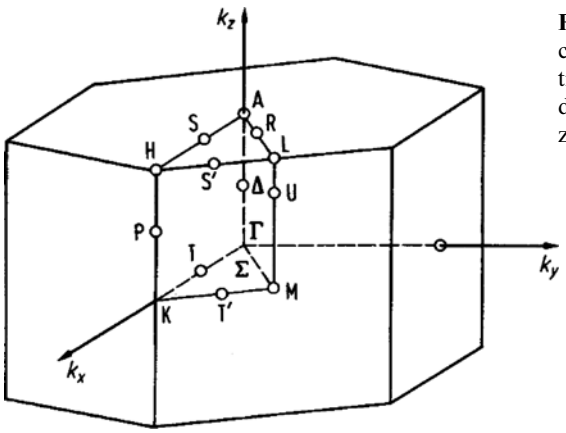

Fig. 1 Brillouin zone corresponding to an hexagonal crystal structure. Beside the typical high symmetry directions (Γ–K–M, Γ–M, and Γ–A), special directions are displayed that correspond to the edges of the Brillouin zone.

TO and LO modes is smaller than that observed in Raman measurements. The main goal of the present INS measurements was to examine the agreement between theory and experiments for the LO branches for finite momentum transfers, in order to ascertain whether these discrepancies take place just at $q = 0$ or they extend into the Brillouin zone.

Figure 1 shows the Brillouin zone of the wurtzite structure with the main high symmetry directions indicated by solid lines. Previous INS data reported in the literature were obtained for the acoustic branches along the [110] (Γ–K–M), [100] (Γ–M), and [001] (Γ–A) directions. In this work we present data corresponding mainly to the optic branches along several directions, among them the [1/2 0 q]

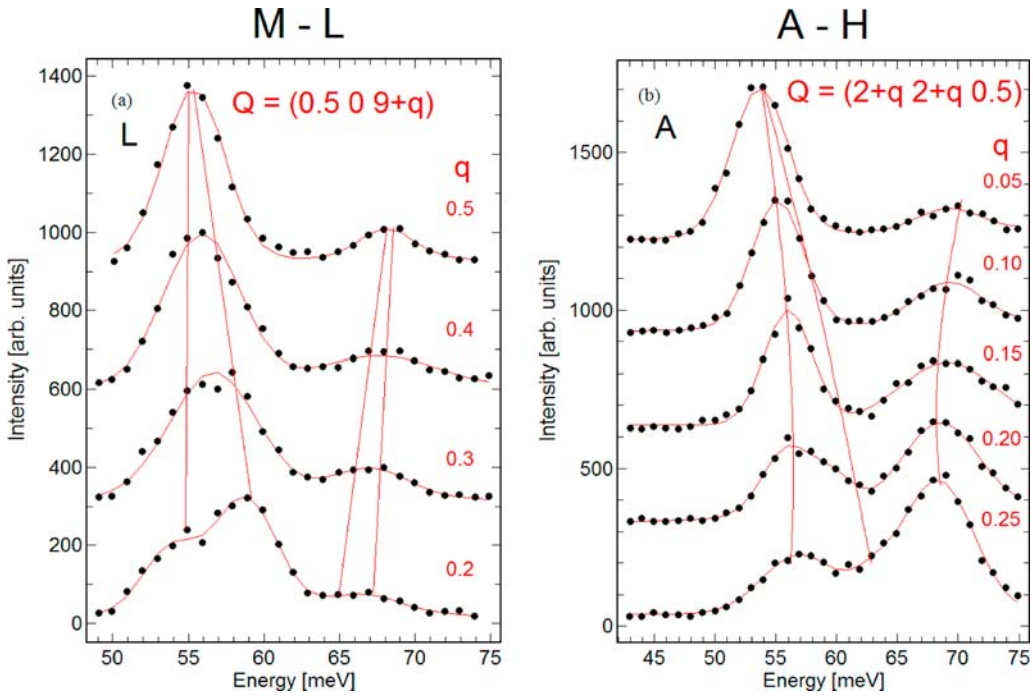

Fig. 2 (online colour at: www.pss-b.com) Selected INS spectra for momentum transfers along the boundaries of the Brillouin zone: (a) [0.5 0 q] direction (M–L), and (b) [q q 0.5] direction (A–H). The red curves display least-squares fits with Gaussian profiles and the lines crossing the spectra are guides to the eye to indicate the energy of the different modes.

(L–M) and the [1/3 1/3 q] (K–H) that, due to the lower symmetry, should be more sensitive to the details of the calculations. The phonon frequencies calculated in Ref. [10] are compared with the experimental data for these directions.

Selected spectra corresponding to the [q q 0.5] (A–H) and [0.5 0 q] (M–L) directions are shown in Fig. 2. These directions correspond to boundaries of the Brillouin zone where sometimes, e.g. for A–H and A–L directions, the symmetry is increased and the number of modes is therefore normally reduced. Beside the experimental data, Fig. 2 displays guides to the eye corresponding to the frequency of the observed phonons. The phonon frequencies were obtained by fitting the spectra with a least-squares routing using Gaussian profiles.

Figure 3 displays the INS phonon dispersions (solid symbols) compared to the calculated ones (solid curves) for selected high symmetry directions corresponding to the boundaries of the Brillouin zone. There is an overall good agreement between both data sets.

The INS data for the acoustic modes at the high symmetry points (K, H, A, L, M) agree very well with the calculated frequencies, the only exception being the lower acoustic branch at the A- and M-points. This branch originates at the lower E_2 mode of the Γ-point, which also showed discrepancies between the calculations and previous INS data (see Ref. [10] for comparison). Concerning the optical phonons, the situation is more complicated. The spectral resolution (4 meV) allows us to ascertain the optical phonon frequencies with an accuracy better than 1 meV. Whereas some directions show an excellent agreement between theory and experiment, e.g. K–H and H–A, there are significant differences for TO and LO modes along the L–M direction, especially at the M-point. These discrepancies are consistent with those observed when comparing the calculations with Raman data [10]: The E_1^{LO} and A_1^{LO} frequencies are underestimated whereas the A_1^{TO} mode, which is obtained by continuation of the lowest optical branch going from M to Γ, is overestimated by the calculation. The fact that there is a common trend in these differences and the good agreement obtained for other directions allows us to reduce the possible sources for these discrepancies. The experimental data, both Raman and INS, were obtained at low temperature, so we can exclude temperature effects in these deviations. The only possibility is a deficient theoretical description of the splitting between transverse and longitudinal optic modes, which is given by the well-known Lyddane–Sachs–Teller relation

$$\omega_{LO}^2 - \omega_{TO}^2 = \frac{4\pi Z^{*2}}{V_0 \mu \varepsilon_\infty}. \tag{1}$$

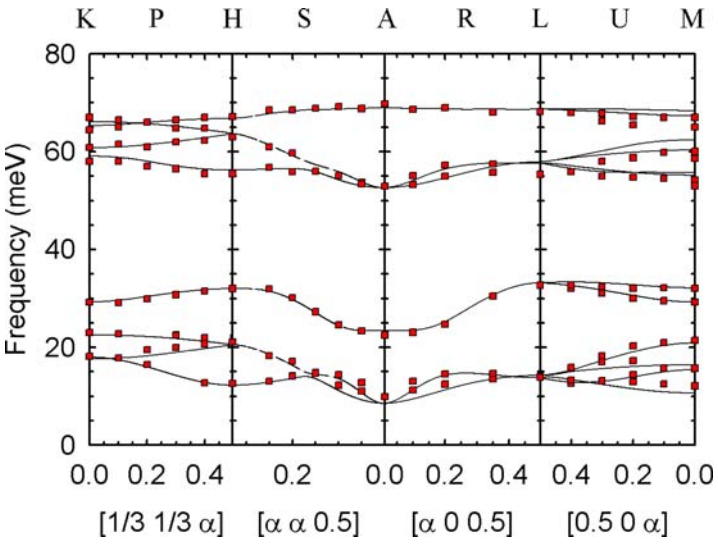

Fig. 3 (online colour at: www.pss-b.com) Phonon dispersion relations of wurtzite ZnO for the main symmetry directions along the boundaries of the Brillouin zone. INS data are displayed by solid squares (red) whereas the calculated phonon dispersions are shown by the solid lines.

The examination of the factors contributing to this splitting yields two possible sources of discrepancy, as shown in Eq. (1): the transverse effective charges Z^* and the dielectric constant ε_∞ (V_0 and μ stand for the volume and reduced mass in the primitive cell, respectively). The calculated values of Z^* are in good agreement with the experimental data [10]. However, the *ab-initio* values of ε_∞ (5.36 and 4.47 along directions parallel and perpendicular to the *c*-axis) used for the phonon calculations are significantly different compared to those deduced from measurements of the refractive index (4.11 and 4.03) [19]. Therefore we can attribute the discrepancies between INS (and Raman) data and the calculated frequencies to inaccuracies in the calculation of the dielectric constant.

5 Conclusions

We have reported INS measurements of the acoustic and optic phonon dispersion relations of wurtzite ZnO along several high symmetry directions. An excellent agreement is found between the experimental data and those of *ab-initio* calculations previously reported in the literature. The discrepancies observed in Ref. [10] are therefore limited to the TO and LO branches close to the Γ-point, whereas lower symmetry directions result unaffected. These discrepancies can be tentatively explained by an inaccurate description of the dielectric tensor and the electronic band gap, as reported in Ref. [10], which in turn hinders a proper calculation of the macroscopic electric field thus changing the frequency of the longitudinal optic phonons. The calculated phonon DOS, however, is in very good agreement with the experimental one [10], since it depends on the accuracy of the global description of the phonon dispersion relations. This explains also the excellent agreement achieved in the comparison between experimental and calculated thermodynamical properties, such as the dependence of the heat capacity on the isotopic mass for ZnO [20]. A more detailed analysis of the whole phonon dispersion relations will be published elsewhere.

Acknowledgement F.J.M. thanks the financial support from the "Programa de Incentivo a la Investigación" of the Universidad Politécnica de Valencia. A.H.R. is supported by the project J-42647-F from CONACYT-Mexico.

References

[1] S. Nakamura, T. Mukai, and M. Senoh, Appl. Phys. Lett. **64**, 1687 (1994).
[2] Ü. Özgür, Y. I. Alivov, C. Liu, A. Teke, M. A. Reshchikov, S. Doğan, V. Avrutin, S. J. Cho, and H. Morkoç, J. Appl. Phys. **98**, 041301 (2005).
[3] A. W. Hewat, Solid State Commun. **8**, 187 (1970).
[4] W. Wegener and S. Hautecler, Phys. Lett. A **31**, 2 (1970).
[5] K. Thoma, B. Dorner, G. Duesing, and W. Wegener, Solid State Commun. **15**, 1111 (1974).
[6] T. C. Damen, S. P. S. Porto, and B. Tell, Phys. Rev. **142**, 570 (1966).
[7] S. P. S. Porto, B. Tell, and T. C. Damen, Phys. Rev. Lett. **16**, 450 (1966).
[8] J. M. Calleja and M. Cardona, Phys. Rev. B **16**, 3753 (1977).
[9] B. H. Bairamov, A. Heinrich, G. Irmer, V. V. Toporov, and E. Ziegler, phys. stat. sol. (b) **119**, 227 (1983).
[10] J. Serrano, A. H. Romero, F. J. Manjón, R. Lauck, M. Cardona, and A. Rubio, Phys. Rev. B **69**, 094306 (2004).
[11] X. Gonze, J.-M. Beuken, R. Caracas, F. Detraux, M. Fuchs, G.-M. Rignanese, L. Sindic, M. Verstraete, G. Zerah, F. Jollet, M. Torrent, A. Roy, M. Mikami, Ph. Ghosez, J.-Y. Raty, and D. C. Allan, Comput. Mater. Sci. **25**, 478–492 (2002).
[12] N. Trouiller and J. L. Martins, Phys. Rev. B **43**, 1993 (1991).
[13] S. Baroni, P. Gianozzi, and A. Testa, Phys. Rev. Lett. **58**, 1861 (1987).
[14] X. Gonze and C. Lee, Phys. Rev. B **55**, 10355 (1997).
[15] D. L. Rousseau, R. P. Bauman, and S. P. S. Porto, J. Raman Spectrosc. **10**, 253 (1981).
[16] C. A. Argüello, D. L. Rousseau, and S. P. S. Porto, Phys. Rev. **181**, 1351 (1969).
[17] J. Serrano, F. J. Manjón, A. H. Romero, F. Widulle, R. Lauck, and M. Cardona, Phys. Rev. Lett. **90**, 055510 (2003).
[18] F. J. Manjón, B. Marí, J. Serrano, and A. H. Romero, J. Appl. Phys. **97**, 053516 (2005).
[19] K. Vedam and T. A. Davis, Phys. Rev. **181**, 1196 (1969).
[20] J. Serrano, R. K. Kremer, M. Cardona, G. Siegle, A. H. Romero, and R. Lauck, Phys. Rev. B **73**, 094303 (2006).

